

JOINT MAP TIME AND FREQUENCY SYNCHRONIZATION IN PRESENCE OF IMPERFECT CHANNEL STATE INFORMATION

Cong Luong Nguyen¹, Anissa Mokraoui¹, Pierre Duhamel², Nguyen Linh-Trung³

¹L2TI, Institut Galilée, Université Paris 13, Sorbonne Paris Cité
99 Avenue J.-B Clément, F93430 Villetaneuse, France

²LSS/CNRS, SUPELEC, 3 rue Joliot Curie, F91192 Gif sur Yvette, France

³VNU University of Engineering and Technology, 144 Xuan Thuy, Cau Giay, Hanoi, Vietnam
{luong.nguyen, anissa.mokraoui}@univ-paris13.fr, pierre.duhamel@lss.supelec.fr, linhtrung@vnu.edu.vn

ABSTRACT

This paper deals with synchronization problem in IEEE 802.11a wireless system. In addition to traditional training sequences, the SIGNAL field of the physical frame can be considered as a new source of information. Indeed the receiver is able to predict the SIGNAL unknown parts relying on the knowledge provided by the CSMA/CA protocol during the negotiation of the transmission medium reservation. The exchanged RtS control frame used jointly with the bit-rate adaptation algorithm to the channel helps the receiver not only to predict the SIGNAL field but also to get information on the channel state. Based on this knowledge, joint MAP channel, time and frequency synchronization algorithm is carried out. Moreover to estimate the residual time offset, a timing metric in frequency domain is performed by minimizing the average of transmission errors in the presence of all channel estimation errors. The performance in terms of probability of synchronization failure is shown to be improved compared to existing algorithms.

Index Terms— IEEE 802.11a, time synchronization, frequency synchronization, CSMA/CA, RtS

1. INTRODUCTION

Relying on Orthogonal Frequency Division Multiplexing (OFDM) technique, IEEE 802.11a standard supports a high-speed data transmission [1]. However the main disadvantage of this technique is its sensitivity to the Inter-Symbol Interference (ISI) and Inter-Carrier Interference (ICI) in case of time or frequency synchronization errors [2]. An accurate time and frequency synchronization is needed at the receiver. It can be performed either on redundant information (Non-Data-Aided (NDA) techniques) or training sequences (Data-Aided (DA) techniques) included in the transmitted physical packet.

NDA approaches usually employ a Cyclic Prefix (CP) which is a copy of the OFDM symbol data part. The correlation property between the CP and its copy in OFDM symbol is then exploited for time synchronization ([3], [4], [5], [p.163, [6]], frequency synchronization ([7], [p.170, [6]]) or both time and frequency synchronization ([8], [9], [10], [11]). For time and frequency synchronization, a Maximum Likelihood (ML) function is commonly used.

DA algorithms exploit training sequences either designed by authors (see e.g. [12], [13]) or specified by some standards (see e.g. [14], [15]). In [16], a joint Carrier Frequency Offset (CFO) and

channel estimation using Maximum-A-Posteriori (MAP) criterion is developed. In [17], a Fine Time Synchronization (FTS) is performed jointly with channel estimation based on the relationship between time offset and channel estimation process.

Given advantages of NDA and DA approaches, this paper combines these two approaches. This strategy has already been developed in [18], [19], [20] for time synchronization and in [21] for time and frequency synchronization adapted to IEEE 802.11a wireless system. To improve the performance of the developed algorithm in [21], we propose a multistage time and frequency synchronization algorithm in presence of imperfect channel state information.

The results provided in [17], [18], [19], show that the channel estimation strategy strongly impacts the timing recovery accuracy. Therefore rather than trying to find the best channel estimator, we derive a timing metric minimizing the average of the transmission error probability over channel estimation errors. This paper is organized as follows. Next section introduces the IEEE 802.11a wireless communication system. Section 3 concerns the proposed time and frequency synchronization algorithm. Section 4 discusses simulation results. Section 5 concludes the work.

2. IEEE 802.11A COMMUNICATION SYSTEM

IEEE 802.11a physical packet is composed of three main fields: the PREAMBLE training field, the SIGNAL field and the DATA field. The PREAMBLE field helps the receiver to synchronize with respect to the transmitter. This field is composed of: (i) ten identical and known Short Training Field (STF) usually used for Automatic Gain Control (AGC), diversity selection, signal detect and Cross Frequency Synchronization (CFS); and (ii) two identical and known Long Training Fields (LTF) reserved for channel estimation and Fine Frequency Synchronization (FFS). The SIGNAL field provides information about the transmission rate and DATA field length. The physical packet modulation is followed by [1].

At the receiver, the discrete baseband signal $r_{\Delta}(n)$ reads

$$r_{\Delta}(n) = \sum_{i=0}^{L-1} h(i)x(n-i-\theta)e^{j\frac{2\pi\epsilon(n-\theta)}{N}} + g(n), \quad (1)$$

where $h(i)$ is the slowly time-varying discrete complex CIR with $\sum_{i=0}^{L-1} E\{|h(i)|^2\} = 1$ (E is the expectation operator); L the number of channel taps; N the number of FFT points; $x(n)$ is the transmitted sample; $g(n)$ the complex AWGN with variance σ_g^2 ; ϵ $= \Delta F_c T$ the normalized CFO with ΔF_c being the carrier frequency

This work was supported by the Ministry of Science and Technology of Vietnam, under project number 39/2012/HD/NDT.

offset between the transmitter and the receiver; T being the OFDM symbol duration; and θ the symbol timing. Estimating the parameters θ and ϵ is the goal of this paper.

3. PROPOSED DA-NDA MULTISTAGE SYNCHRONIZATION ALGORITHM

This section explains how the redundant information that will be exploited by the proposed multistage frame synchronization algorithm summarized in Fig. 1 can be extracted.

3.1. Redundant information at physical layer

The SIGNAL field of the IEEE 802.11a physical frame, composed of two subfields "RATE" and "LENGTH", is considered as redundant information since these subfields can be known if the receiver exploits the knowledge provided by the CSMA/CA (Carrier Sense Multiple Access with Collision Avoidance) protocol when it is triggered. Before sending any information, the transmitter initiates the communication by sending a RtS (Request to Send) control frame to ask the receiver if it is available [22]. If it is the case, the receiver performs a rate adaptation algorithm by measuring the Signal-to-Noise Ratio (SNR) level of the received RtS frame to estimate the channel conditions [24]. Then it replies with a Clear to Send (CtS) control frame in order to: (i) inform other stations (in the same network) of its unavailability to receive information during a specified duration; and (ii) suggest to the transmitter a transmission rate that it should use to transmit its physical data packet. Therefore the receiver has a knowledge of the transmission rate corresponding to the "RATE" subfield value of the SIGNAL field. Subsequently, the unknown "LENGTH" subfield is deduced from the following relationship [1]:

$$\text{LENGTH} = \text{RATE} \times \frac{T_{\text{packet}} - T_{\text{pre}} - T_{\text{SIGNAL}} - (T_{\text{symp}}/2) - 22}{8}, \quad (2)$$

since the "RATE" and the durations (given in micro-seconds) of PREAMBLE (T_{pre}), SIGNAL field (T_{SIGNAL}) and OFDM symbol (T_{symp}) are known values provided in [1]. However the unknown duration T_{packet} required to transmit the DATA physical packet is unknown. We deduce this value from the DURATION field value extracted from the RtS control frame as follows [25]:

$$T_{\text{packet}} = \text{DURATION} - 3T_{\text{SIFS}} - T_{\text{CIS}} - T_{\text{ACK}}, \quad (3)$$

where T_{SIFS} is the known duration of a Short Inter-Frame Space, T_{CIS} and T_{ACK} are respectively the known required durations to transmit CtS and Acknowledgement (ACK) frames. The "Parity" field is then deduced from the "RATE", "LENGTH" and "R" (Reserved) known values and is followed by six zero tail bits to complete the SIGNAL field. This field is now fully recognized by the receiver and is exploited for frame synchronization problem.

3.2. First stage: DA-NDA coarse time synchronization

The first stage recovers coarsely the symbol timing θ of the received signal. For this purpose two steps combining DA and NDA strategies are performed as described below.

3.2.1. Coarse symbol timing recovery

If the transmitted signal is heavily distorted by the wireless channel, the symbol timing based on the Cross-Correlation Function (CCF)

performed between the received signal $r_{\Delta}(n)$ and the known STF $c(n)$ will be affected. To enhance the accuracy of this estimation, the received signal $r_{\Delta}(n)$ in CCF is replaced by its estimation $\hat{x}(n)$ which would be close to the true transmitted signal $x(n)$. To do so, the channel is estimated during the negotiation of transmission medium reservation managed by the CSMA/CA mechanism. Note that RtS and CtS control frames are sent with a power level higher than the nominal transmission power level at which the DATA frame is sent to permit all stations of the same network to hear these control frames [23]. Therefore during the negotiation (i.e. RtS/CtS), the transmitter and receiver are assumed to be correctly synchronized to prepare the transmission of the physical DATA packet. Moreover the channel is assumed to be static between the transmission duration of RtS and DATA frames since the interval time between the transmitted physical packet and RtS control frame is small (in the worst case $T_{\text{RtS}} + T_{\text{CIS}} + 2T_{\text{SIFS}} = 124 \mu\text{s}$ with lowest rate of 6 Mb/s), meaning that Doppler frequency can be considered as a negligible value.

Note that both control (RtS, CtS) and DATA frames use the same PREAMBLE field. As mentioned in the standard for the physical packet, we base the channel estimation on LTF of the RtS PREAMBLE. A MAP-based channel estimation is then considered:

$$\hat{\mathbf{h}} = (\mathbf{Q}^H \mathbf{Q} + \sigma_g^2 \mathbf{R}_{\mathbf{h}}^{-1})^{-1} (\mathbf{Q}^H \mathbf{r}_{\text{RtS}} + \sigma_g^2 \mathbf{R}_{\mathbf{h}}^{-1} \boldsymbol{\mu}_{\mathbf{h}}), \quad (4)$$

where \mathbf{r}_{RtS} is the received RtS frame signal corresponding to the LTF sequence; \mathbf{Q} contains the LTF training samples; σ_g^2 is the noise variance; $\mathbf{R}_{\mathbf{h}}$ is the covariance matrix of the true channel; and $\boldsymbol{\mu}_{\mathbf{h}}$ is the mean vector of the true channel. Instead of using a Power Delay Profile (PDP) to calculate $\mathbf{R}_{\mathbf{h}} = E\{\mathbf{h}\mathbf{h}^H\}$, we replace the true channel \mathbf{h} by its LS estimation $\hat{\mathbf{h}}$ given by the IFFT of $\hat{\mathbf{H}} = \mathbf{X}^{-1} \mathbf{R}_{\text{RtS}}$ with \mathbf{X} being the diagonal matrix whose elements are the known LTF symbols and \mathbf{R}_{RtS} being the received symbol vector.

Let $\hat{H}(k)$ (with $0 \leq k \leq N-1$) be the channel estimate and $R_{\Delta}(k)$ be the received symbols corresponding to the DATA frame signal in frequency domain, then the transmitted symbol estimate, $\hat{X}(k)$, according to a Zero-Forcing (ZF) equalizer, is provided by $\hat{X}(k) = \frac{R_{\Delta}(k)}{\hat{H}(k)}$. Therefore the symbol timing is determined as follows with L_{STF} the length of the known STF sequence $c(n)$:

$$\hat{\theta} = \arg \max_{\theta} \left| \sum_{n=0}^{L_{\text{STF}}-1} c^*(n) \hat{x}(n + \theta) \right|. \quad (5)$$

3.2.2. SIGNAL field improving coarse time symbol recovery

To estimate the remaining time offset (i.e. $\Delta\theta_s = \hat{\theta} - \theta$) as in [18] and [19], the receiver exploits the 802.11a SIGNAL field as an additional training sequence since all parts of this field are completely known. A CCF is performed between the received signal $r_s(n) = \sum_{i=0}^{L-1} h(i)x(n-i-\Delta\theta_s)e^{j2\pi\epsilon(n-\Delta\theta_s)/N} + g(n)$ and the known SIGNAL field $c_s(n)$ of length L_{SIG} (i.e. CP length added to SIGNAL length). The remaining time offset corresponds to the index among the set of possible values $\Theta = \{\Delta\theta_s^{(k)} | k = -K, \dots, K; K \in \mathbf{N}\}$ which maximizes the CCF absolute value as follows:

$$\Delta\hat{\theta}_s = \arg \max_{\Delta\theta_s^{(k)} \in \Theta} \left| \sum_{n=0}^{L_{\text{SIG}}-1} c_s^*(n) r_s(n + \Delta\theta_s^{(k)}) \right|. \quad (6)$$

After this step, the received signal with a possible remaining time offset $\Delta\theta = \Delta\hat{\theta}_s - \Delta\theta_s$ becomes

$$r_f(n) = \sum_{i=0}^{L-1} h(i)x(n-i-\Delta\theta)e^{j\frac{2\pi\epsilon(n-\Delta\theta)}{N}} + g(n). \quad (7)$$

3.3. Second stage: Joint MAP frequency and time offsets estimation

This stage estimates the possible remaining time offset $\Delta\theta$ and normalized frequency offset ϵ in equation (7) according to a joint MAP frequency and time offsets estimation. To do so, we not only adapt the frequency synchronization algorithm developed in [16] to the IEEE 802.11a specifications but also make changes to the algorithm since the authors assumed that time offset was perfectly compensated. Knowledge of the SIGNAL field is also taken into account at this stage as described above.

The received signal \mathbf{r} corresponding to the two LTF repetitions and SIGNAL field is expressed in matrix form as follows:

$$\mathbf{r} = \Phi_{\Delta\theta,\epsilon} \mathbf{S}_{\Delta\theta} \mathbf{h} + \mathbf{g}, \quad (8)$$

where $\mathbf{r} = [r_f(n), \dots, r_f(n + 2N + N_G + N_S - 1)]^T$; $\mathbf{S}_{\Delta\theta} = [\mathbf{S}_{0,\Delta\theta}, \dots, \mathbf{S}_{L-1,\Delta\theta}]$; $\mathbf{S}_{l,\Delta\theta} = [x(n-l-\Delta\theta), \dots, x(n+2N+N_G+N_S-1-l-\Delta\theta)]^T$; $\mathbf{h} = [h(0), h(1), \dots, h(L-1)]^T$; $\mathbf{g} = [g(n-\Delta\theta), \dots, g(n-\Delta\theta+2N+N_S+N_G-1)]^T$; and $\Phi_{\Delta\theta,\epsilon} = \text{diag} \left\{ e^{j \frac{2\pi\epsilon(n-\Delta\theta)}{N}}, \dots, e^{j \frac{2\pi\epsilon(n-\Delta\theta+2N+N_S+N_G-1)}{N}} \right\}$ with $x(n)$ the known LTF and SIGNAL samples in time domain; N the number of samples of one LTF repetition; N_S the SIGNAL field length and N_G the GI length. \mathbf{h} and \mathbf{g} are the CIR and noise vectors. The unknown parameters $\Delta\theta$, ϵ and \mathbf{h} are jointly estimated according to the MAP criterion as follows:

$$\{\hat{\mathbf{h}}, \hat{\Delta\theta}, \hat{\epsilon}\} = \arg \max_{\mathbf{h}, \Delta\theta, \epsilon} \ln P(\mathbf{h}, \Delta\theta, \epsilon | \mathbf{r}), \quad (9)$$

where P is a *a posteriori* probability density function of \mathbf{h} , $\Delta\theta$ and ϵ given \mathbf{r} . Note that ϵ is also assumed to be uniformly distributed in the range $[-\epsilon_0, \epsilon_0]$.

To solve this equation, a set Λ containing $2M+1$ possible time offset values $\Lambda = \{-\Delta\theta_M, \dots, \Delta\theta_M\}$ is defined. For a given value $\Delta\theta_m \in \Lambda$, the MAP-based estimates of the CFO and channel coefficients are performed according to this expression

$$\{\hat{\mathbf{h}}_{\Delta\theta_m}, \hat{\epsilon}_{\Delta\theta_m}\} = \arg \min_{\mathbf{h}, \epsilon} f_{\text{MAP}}^{(m)}(\mathbf{h}, \epsilon), \quad (10)$$

where $\mathbf{r}_{\Delta\theta_m}$ is the received signal with the offset value $\Delta\theta_m$ and $f_{\text{MAP}}^{(m)}(\mathbf{h}, \epsilon) = \frac{1}{\sigma_g^2} \|\mathbf{r}_{\Delta\theta_m} - \Phi_{\Delta\theta_m,\epsilon} \mathbf{S}_{\Delta\theta_m} \mathbf{h}\|^2 + \mathbf{h}^H \mathbf{R}_{\mathbf{h}}^{-1} \mathbf{h}$. Setting the gradient vector of $f_{\text{MAP}}^{(m)}(\mathbf{h}, \epsilon)$ with respect to \mathbf{h}^H to zero produces the channel estimate as follows:

$$\hat{\mathbf{h}}_{\Delta\theta_m} = [\mathbf{S}_{\Delta\theta_m}^H \mathbf{S}_{\Delta\theta_m} + \sigma_g^2 \mathbf{R}_{\mathbf{h}}^{-1}]^{-1} \mathbf{S}_{\Delta\theta_m}^H \Phi_{\Delta\theta_m,\epsilon}^H \mathbf{r}_{\Delta\theta_m}. \quad (11)$$

Replacing equation (11) into equation (10) results in the following CFO estimate:

$$\hat{\epsilon}_{\Delta\theta_m} = \arg \min_{\epsilon} g_{\text{MAP}}^{(m)}(\epsilon), \quad (12)$$

where $g_{\text{MAP}}^{(m)}(\epsilon) = \mathbf{r}_{\Delta\theta_m}^H \Phi_{\Delta\theta_m,\epsilon} \mathbf{S}_{\Delta\theta_m}^+ \Phi_{\Delta\theta_m,\epsilon}^H \mathbf{r}_{\Delta\theta_m}$, with $\mathbf{S}_{\Delta\theta_m}^+ = \mathbf{S}_{\Delta\theta_m} [\mathbf{S}_{\Delta\theta_m}^H \mathbf{S}_{\Delta\theta_m} + \mathbf{R}_{\mathbf{h}}^{-1} \sigma_g^2]^{-1} \mathbf{S}_{\Delta\theta_m}^H$. Newton-Raphson iterations are applied to estimate $\hat{\epsilon}_{\Delta\theta_m}$. To ensure the convergence of algorithm, the initial starting frequency offset point $\hat{\epsilon}_{\Delta\theta_m,0}$ is taken as the coarse value close to the true frequency offset provided by the Auto-Correlation Function (ACF) as mentioned in references [14] and [15]. Substituting $\hat{\epsilon}_{\Delta\theta_m}$ into equation (11) gives the CIR estimate as follows:

$$\hat{\mathbf{h}}_{\Delta\theta_m} = [\mathbf{S}_{\Delta\theta_m}^H \mathbf{S}_{\Delta\theta_m} + \sigma_g^2 \mathbf{R}_{\mathbf{h}}^{-1}]^{-1} \mathbf{S}_{\Delta\theta_m}^H \Phi_{\Delta\theta_m,\hat{\epsilon}_{\Delta\theta_m}}^H \mathbf{r}_{\Delta\theta_m}. \quad (13)$$

Among the $2M+1$ estimates of $\hat{\mathbf{h}}_{\Delta\theta_m}$, we select the one that satisfies the following conditions:

$$|\hat{h}_{\Delta\theta_m}(0)| > \beta \max_{\Delta\theta_i} |\hat{h}_{\Delta\theta_i}(0)|, \quad (14)$$

where β is a given threshold selected according to the noise level and type of channel model. The set Λ now becomes $\Gamma = \{\omega_0, \dots, \omega_{M'}\}$; $M' \leq 2M$ and finally, the correct time offset is estimated by

$$\Delta\hat{\theta} = \arg \max_{\omega_{m'}} \sum_{n=0}^{L-1} |\hat{h}_{\omega_{m'}}(n)|^2. \quad (15)$$

3.4. Third stage: Remaining time offset recovery using transmission error function average over channel estimation errors

Assume that frequency offset is completely compensated but a possible time offset still remains $\Delta\theta_e = \Delta\hat{\theta} - \Delta\theta$. The received signal in frequency domain is expressed as follows:

$$\mathbf{R}_e = \mathbf{X}\mathbf{H} + \mathbf{G}, \quad (16)$$

where \mathbf{G} is the noise vector of size $N \times 1$. \mathbf{H} is the true CIR in frequency domain assumed to follow a circular Gaussian distribution with zero mean $\Psi(\mathbf{H})$. A key point in improving the performance of the estimation is to use accuracy statistic. In this section, a conditional PDF $\Psi(\mathbf{H}|\hat{\mathbf{H}})$, with $\hat{\mathbf{H}} = \mathbf{X}^{-1}\mathbf{R}_e$, is taken into account in the computation of estimate of the time offset. The remaining time offset to be estimated is considered to the one which minimizes the following new metric:

$$\Delta\hat{\theta}_e = \arg \min_{\Delta\theta_e \in \Lambda} \{\tilde{D}(\Delta\theta_e)\}, \quad (17)$$

where $\tilde{D}(\Delta\theta_e)$ is the average of Transmission Error Function over all Channel Estimation Errors (TEF average over CEE) given by:

$$\tilde{D}(\Delta\theta_e) = E_{\mathbf{H}|\hat{\mathbf{H}}} [D(\mathbf{H})] = \int_{\mathbf{H}} D(\mathbf{H}) \Psi(\mathbf{H}|\hat{\mathbf{H}}) d(\mathbf{H}), \quad (18)$$

where $D(\mathbf{H}) = \|\mathbf{R}_e - \mathbf{X}\mathbf{H}\|^2$. The form of equation (18) has been inspired from [26]. To solve this equation, the knowledge of $\Psi(\mathbf{H}|\hat{\mathbf{H}})$ PDF is required and is given by $\Psi(\mathbf{H}|\hat{\mathbf{H}}) = \frac{\Psi(\hat{\mathbf{H}}|\mathbf{H})\Psi(\mathbf{H})}{\Psi(\hat{\mathbf{H}})}$, where $\Psi(\hat{\mathbf{H}}|\mathbf{H}) \sim \mathcal{CN}(\mu_{\hat{\mathbf{H}}|\mathbf{H}}, \Sigma_{\hat{\mathbf{H}}|\mathbf{H}})$ and $\Psi(\hat{\mathbf{H}}) \sim \mathcal{CN}(\mu_{\hat{\mathbf{H}}}, \Sigma_{\hat{\mathbf{H}}})$. Specifically $\mu_{\hat{\mathbf{H}}|\mathbf{H}} = E\{\hat{\mathbf{H}}|\mathbf{H}\} = E\{\mathbf{H}|\mathbf{H}\} = \mu_{\mathbf{H}} = 0$; and $\Sigma_{\hat{\mathbf{H}}|\mathbf{H}} = E\{\hat{\mathbf{H}}\hat{\mathbf{H}}^H|\mathbf{H}\} = \Sigma_{\epsilon}$ where \mathbf{I} is $N \times N$ identity matrix. In the same way, we obtain $\Psi(\hat{\mathbf{H}}) \sim \mathcal{CN}(\mu_{\hat{\mathbf{H}}}, \Sigma_{\hat{\mathbf{H}}}) = \mathcal{CN}(0, \mathbf{R}_{\mathbf{H}} + \Sigma_{\epsilon})$ where $\mathbf{R}_{\mathbf{H}} = E\{\mathbf{H}\mathbf{H}^H\}$ is deduced from the MAP channel estimate (see equation (4)) $\mathbf{R}_{\mathbf{H}} \approx E\{\hat{\mathbf{H}}_{MAP} \hat{\mathbf{H}}_{MAP}^H\}$. Therefore, we deduce $\Psi(\mathbf{H}|\hat{\mathbf{H}}) \sim \mathcal{CN}(\mu_{\mathbf{H}|\hat{\mathbf{H}}}, \Sigma_{\mathbf{H}|\hat{\mathbf{H}}})$ with $\mu_{\mathbf{H}|\hat{\mathbf{H}}} = \Sigma_{\Delta} \hat{\mathbf{H}}$ and $\Sigma_{\mathbf{H}|\hat{\mathbf{H}}} = \Sigma_{\Delta} \Sigma_{\epsilon}$ where $\Sigma_{\Delta} = \mathbf{R}_{\mathbf{H}}(\mathbf{R}_{\mathbf{H}} + \Sigma_{\epsilon})^{-1}$. For simplicity, equation (18) is reduced to the following calculation:

$$\tilde{D}(\Delta\theta_e) = E_{\mathbf{W}} [D(\mathbf{W})] = \int_{\mathbf{W}} D(\mathbf{W}) \Psi(\mathbf{W}) d(\mathbf{W}), \quad (19)$$

where $\mathbf{W} \sim \Psi(\mathbf{W}) = \mathcal{CN}(\mu_{\mathbf{H}|\hat{\mathbf{H}}}, \Sigma_{\mathbf{H}|\hat{\mathbf{H}}})$ and $D(\mathbf{W}) = \|\mathbf{R}_e - \mathbf{X}\mathbf{W}\|^2$. After some mathematical manipulations, we obtain

$$\begin{aligned} \tilde{D}(\Delta\theta_e) &= E[\mathbf{R}_e^H \mathbf{R}_e] - E[\mathbf{R}_e^H \mathbf{X}] \mu_{\mathbf{H}|\hat{\mathbf{H}}} - \mu_{\mathbf{H}|\hat{\mathbf{H}}}^H E[\mathbf{X}^H \mathbf{R}_e] + \\ &+ \text{tr}(\Sigma_{\mathbf{H}|\hat{\mathbf{H}}} \mathbf{X} \mathbf{X}^H) + \mu_{\mathbf{H}|\hat{\mathbf{H}}}^H \mathbf{X}^H \mathbf{X} \mu_{\mathbf{H}|\hat{\mathbf{H}}}, \end{aligned} \quad (20)$$

where $\text{tr}(\cdot)$ indicates the trace operator. The remaining time offset $\Delta\hat{\theta}_e$ is then deduced from equation (17).

4. PERFORMANCE ANALYSIS

IEEE 802.11a simulation parameters are as follows: bandwidth $B = 20$ MHz; sampling time $T_s = 50$ ns; number of subcarriers $N_c = 52$; number of points FFT/IFFT $N = 64$; subcarrier spacing $\Delta F_c = 0.3125$ MHz; data rate of 6 Mbps; $L_{STF} = 160$; $L_{SIG} = 80$; $K = 80$ and $M = 30$ [1]. For a carrier frequency $f_c = 5.2$ GHz and an OFDM symbol duration $T = N \times T_s = 3.2$ μ s, the normalized CFO (i.e. ϵ) falls in the range $[-0.6, 0.6]$. ϵ and θ are taken randomly according to a uniform distribution. Simulation results are performed under BRAN-A (CH-A) channel model [27].

Fig. 2 provides the MSE between the true CFO and its estimate ($E\{(\epsilon - \hat{\epsilon})^2\}$) versus SNR (Signal-to-Noise Ratio). The curves show that regardless of time synchronization being perfect (known perfectly by the receiver and is then used to perfectly compensate the time offset, i.e. "proposed algo. with a perfect TS") or not (i.e. "proposed algo."), the MSE of our algorithm is much lower than Canet's algorithm ([15]). Moreover, the two curves associated to our algorithm are similar showing that the estimated time offset is well performed since it is similar to a perfect time offset compensation.

Fig. 3 measures the detection probability of arrival time of the transmitted physical packet (denoted as P_d) for a given deviation with respect to its true time position (i.e. $\hat{\theta} - \theta$) at SNR=15 dB using 10^7 realizations. The proposed algorithm achieves the highest estimation accuracy of 99% when the packet arrival time is detected without time deviation compared to other algorithms developed in [15] and [21]. Indeed, for a given deviation equal to zero, it is illustrated that $P_d(\text{Algo. in [15]})=0.51$, $P_d(\text{Algo. in [21]})=0.991$, $P_d(\text{Proposed algo.})=0.997$.

Fig. 4 measures the Probability of Synchronization Failure (PSF) versus SNR. It is possible to accept packets whose arrival time is estimated after the true position with a time deviation (different from zero) due to the use of CP [28]. Indeed, according to the selected channel model, we can accept arrival packet with a delay no more than 7 samples (i.e. $\hat{\theta}_{\text{new}} = \hat{\theta} - 7$). With or without time deviation, the PSF of the proposed algorithm is smaller than that of other algorithms ([15], [21]). Moreover, the curves associated to our algorithm are similar showing that the estimated frequency offset is well performed since it is similar to a perfect frequency offset compensation.

The question of whether the estimated transmission channel \hat{h} (see Section 3.2.1) during the transmission medium negotiation may change when DATA is allowed to be transmitted when stations move is addressed. In the worst case, since the maximum Doppler frequency f_D is equal to 26 Hz (with walking speed of 1.5 m/s, carrier frequency of 5.2 GHz, rate of 6 Mb/s) the estimated channel is not affected [22]. This is confirmed by simulation results of the "proposed algo. (Doppler freq., deviation ≤ 7 ") which are close to the case with no Doppler frequency (see Fig. 4).

5. CONCLUSION

Based on DA and NDA approaches, this paper proposed time and frequency synchronization algorithm adapted to IEEE 802.11a wireless network. In addition to information dedicated to synchronize mobile stations, redundant information extracted at physical layer has been retained since the receiver is able to predict this information involving the CSMA/CA mechanism when it is triggered. Moreover the exchanged control frame (RtS), combined to bit-rate adaptation algorithm to the channel, is exploited to estimate the transmission channel before the first algorithm stage. To obtain a more precise

estimate of time offset, we performed additionally the timing metric which is further also exploited in the other DA-based systems. The multistage synchronization approach achieves significant improvement in terms of PSF in indoor environment.

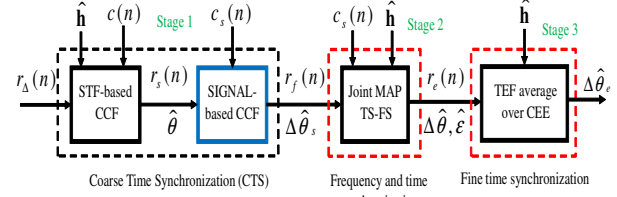


Fig. 1. Proposed DA-NDA multistage synchronization algorithm.

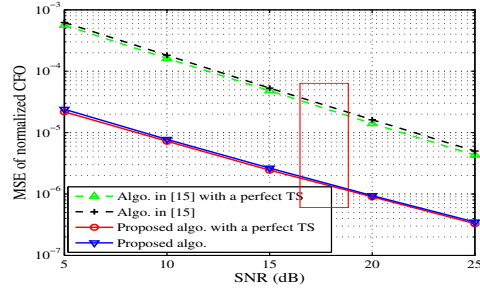


Fig. 2. MSE of normalized CFO.

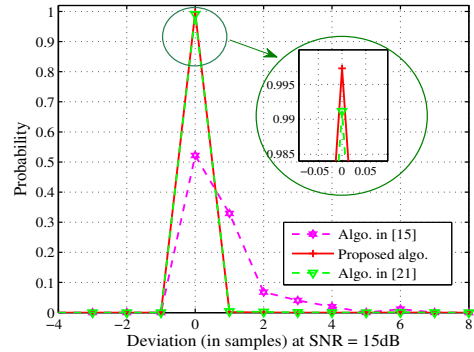


Fig. 3. Deviation with respect to physical packet true time position.

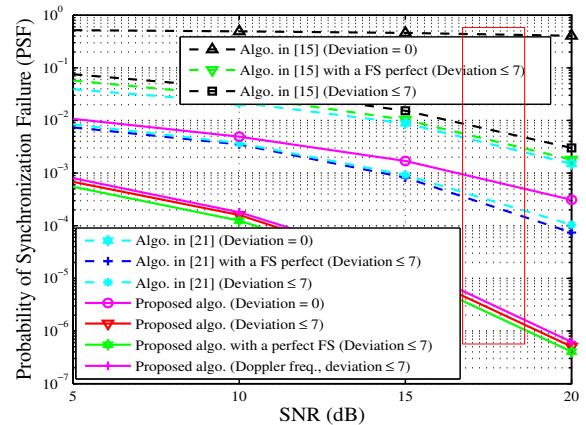


Fig. 4. PSF under BRAN-A channel model.

6. REFERENCES

- [1] "IEEE Std.802.11a," 1999.
- [2] T. Pollet, M. V. Bladel, and M. Moeneclaey, "BER sensitivity of OFDM systems to carrier frequency offset and Wiener phase noise," *IEEE Trans. Commun.*, vol. 43, pp. 887–895, 1995.
- [3] M. Speth, F. Classen, and H. Meyr, "Frame synchronization of OFDM systems in frequency selective fading channels," In *IEEE VTC'97*, vol. 3, pp. 1807–1811, May 1997.
- [4] Ph. J. Tourtier, R. Monnier, and P. Lopez, "Multicarrier modem for digital HDTV terrestrial broadcasting," *Signal processing: Image communication*, pp. 379–403, 1993.
- [5] J. J. van de Beek, M. Sandell, M. Isaksson, and P. O. Borjesson, "Low-complex frame synchronization in OFDM systems," *Proc. IEEE Int. Conf. Universal Personal Commun.*, pp. 982–986, Nov. 1995.
- [6] Y. S. Cho, J. Kim, W. Y. Yang, and C. G. Kang, *MIMO-OFDM Wireless Communications with MATLAB*. John Wiley & Sons, 2010.
- [7] N. Benvenuto and S. Tomasin, "On the comparison between OFDM and single carrier modulation with a DFE using a frequency-domain feedforward filter," *IEEE Trans. Commun.*, pp. 947–955, 2002.
- [8] S. Ma, X. Pan, G. H. Yang and T. S. Ng, "Blind Symbol Synchronization Based on Cyclic Prefix for OFDM Systems," *IEEE Trans. Vehicular Technology*, vol. 58, pp. 1746–1751, 2009.
- [9] B. Park, E. Ko, H. Cheon, C. Kang, and D. Hong, "A blind OFDM synchronization algorithm based on Cyclic correlation," *Proc. IEEE Global Telecom. Conf.*, pp. 3116–3119, Nov. 2001.
- [10] J. J. Van de Beek, M. Sandell, and P. O. Borjesson, "ML estimation of time and frequency offset in OFDM systems," *IEEE Trans. Signal Processing*, pp. 1800–1805, 1997.
- [11] M. Sandell, J. J. Van de Beek, and P. O. Borjesson, "Timing and frequency synchronization in OFDM systems using the cyclic prefix," In *Proc. Int. Symp. Synchronization*, pp. 16–19, 1995.
- [12] T. M. Schmidl and D. C. Cox, "Robust frequency and timing synchronization for OFDM," *IEEE Trans. Commun.*, vol. 45, pp. 1613–1621, Dec. 1997.
- [13] B. Y. Prasetyo, F. Said, and A. H. Aghvami, "Fast burst synchronisation technique for OFDM-WLAN systems," *IEEE Proc. Commun.*, pp. 292–297, Oct. 2000.
- [14] S. K. Manusani, R. S. Kshetrimayum, and R. Bhattacharjee, "Robust time and frequency synchronization in OFDM based 802.11a WLAN systems," *IEEE Trans. Commun.*, pp. 1–4, Sep. 2006.
- [15] M. J. Canet, V. Almenar, J. Marin-Roig, and J. Valls, "Time synchronization for the IEEE 802.11a/g WLAN standard," *PIMRC*, pp. 1–5, 2007.
- [16] H. Nguyen-Le, T. Le-Ngoc, "Pilot-Aided Joint CFO and Doubly-Selective Channel Estimation for OFDM Transmissions," *IEEE Trans. Sig. Proc.*, vol. 56, pp. 514–522, Dec. 2010.
- [17] Y. Zhang, J. Zhang, and M. Xia, "Joint timing synchronization and channel estimation for OFDM systems via MMSE criterion," *IEEE VTC 2008 Fall*, pp. 1–4, 2008.
- [18] C. L. Nguyen, A. Mokraoui, P. Duhamel, and N. Linh-Trung, "Time Synchronization Algorithm in IEEE 802.11a Communication System," *EUSIPCO*, Aug. 2012.
- [19] C. L. Nguyen, A. Mokraoui, P. Duhamel, and N. Linh-Trung, "Enhanced Time Synchronization for IEEE 802.11a System Using SIGNAL Field And MAP Channel Estimation," *International Conf. on Advanced Technologies for Commun.*, 2012.
- [20] C. L. Nguyen, A. Mokraoui, P. Duhamel, and N. Linh-Trung, "Improved Time Synchronization in Presence of Imperfect Channel State Information," *IEEE ICASSP 2013*, May 26-31, 2013 Vancouver, Canada.
- [21] C. L. Nguyen, A. Mokraoui, P. Duhamel, and N. Linh-Trung, "Improved Time and Frequency Synchronization Algorithm for IEEE 802.11a Wireless Standard Based on SIGNAL field," *REV Journal on Electronics and Comm.*, vol. 3, pp. 40-49, January-June 2013.
- [22] M. Ergen and P. Varaiya, "Throughput Analysis and Admission Control for IEEE 802.11a," *Mobile Networks and Applications*, pp. 705–716, 2005.
- [23] F. R. Gfeller and W. Hirt, "Method for improved wireless optical communication and frames for use in a wireless optical communication system," *U.S. Patent No 6,643,469*. Nov. 2003.
- [24] Z. Li, A. Das, A. K. Gupta and S. Nandi, "Full auto rate MAC protocol for wireless Ad-hoc networks," *IEEE Proceedings on Commun.*, vol. 152, issue 3, pp. 311–319, 2005.
- [25] M. Gast, *802.11 Wireless Networks: The Definitive Guide*, O'Reilly Media; 2nd. ed., 2005.
- [26] P. Piantanida, S. Sadough, and P. Duhamel, "On the outage capacity of a practical decoder accounting for channel estimation inaccuracies," *IEEE Trans. Commun.*, vol. 57, pp. 1341-1350, May 2009.
- [27] Norme ETSI, "Channel models for HIPERLAN/2 in different indoor scenarios," <http://www.etsi.org>, 1998.
- [28] Y. Mostofi and D. C. Cox, "Mathematical analysis of the impact of timing synchronization errors on the performance of an OFDM system," *IEEE Trans. Commun.*, Vol. 54, pp. 226–230, 2006.